

Effect of Receiver Bandwidth on the Amplitude Distribution of VLF Atmospheric Noise^{1, 2}

Forrest F. Fulton, Jr.³

(October 27, 1960; revised November 8, 1960)

The distribution function of envelope voltage for short samples of atmospheric radio noise as received by a communications receiver in the VLF range always shows a marked departure from that obtained for Gaussian noise. If it is considered that this departure is caused by strong noise pulses which do not overlap in time, the effect of changes in the receiver bandwidth on the observed distribution function can be deduced by consideration of the changes in the receiver impulse response. A transformation can be obtained which gives an excellent approximation to the change in a mathematical representation of the distribution function in the range of probabilities below 1 percent. Empirical relationships are suggested which give useful estimates of the change in the distribution function over the total range of probabilities.

1. Introduction

In the VLF range, atmospheric radio noise is one of the important factors in a system design. If all of the manmade interference is controlled by allocation procedures and good engineering, the atmospheric noise provides the ultimate background disturbance from which the desired signal must be separated [CCIR Rpt. 65, ITU, 1957; Watt, Coon, Maxwell, and Plush, 1958]. Studies of the noise must be of a statistical nature, but there are problems which differ, for instance, from those of statistical studies of thermal noise, because the atmospheric noise is a nonstationary process. Since the statistics of the process change with time, the accuracy of measuring statistical parameters cannot be indefinitely increased by increasing the length of time of the measurements. Experience has shown that when measuring the amplitude probability distribution of the noise envelope, samples of noise 10 to 20 min in length are short enough to avoid difficulties due to the nonstationary characteristics of the process, but are long enough to give useful information for system design purposes [Hoff and Johnson, 1952; Watt and Maxwell, 1957].

One of the problems which occurs in system design is determining the percentage of time that the envelope of the noise will exceed the signal level, and how this varies as the receiver bandwidth is changed. In principle this can be calculated precisely if enough is known about the statistics of the noise. An applicable procedure, as described by Widrow [1957], is to consider a sampled version of the input noise for which the joint probability distribution of the samples can be determined, and to use this to calculate the probability distribution of a sampled

version of the filter output. If the sampling rate at the input is high enough, the probability distribution of the output samples will accurately represent the probability distribution of the continuous output. The difficulty with this procedure is that the interval between samples at the input must in general be short relative to the correlation time of the noise [Ragazzini and Franklin, 1958], so that a very high order joint probability density function must be calculated for the filter output. The purpose of this paper is to present a technique which requires much less computation, but gives an accuracy commensurate with the statistical knowledge of the noise.

2. Noise Characteristics

Figure 1 shows two samples of measurements of atmospheric noise envelope distributions, one of relatively high dynamic range conditions and the other of noise of relatively low dynamic range; the dotted

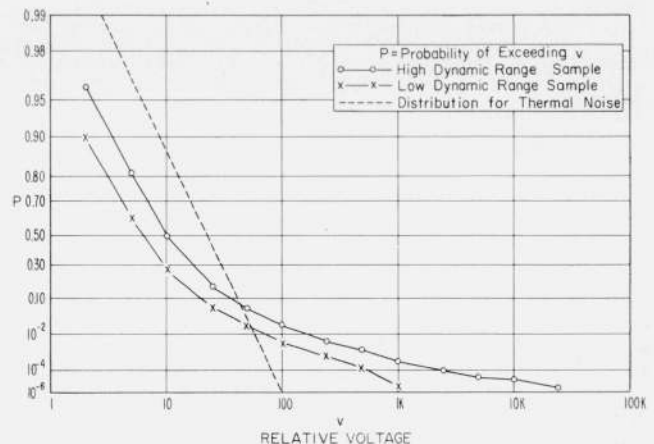


FIGURE 1. Typical measurements of atmospheric noise envelope distribution.

¹Contribution from Central Radio Propagation Laboratory, National Bureau of Standards, Boulder, Colo.

²An earlier version of this paper was presented at the Symposium on VLF Radio Waves held in Boulder, Colo., January 1957.

³Present address: Lockheed Aircraft Corporation, Palo Alto, Calif.

line represents the measurement which is obtained for thermal noise. At the low voltages which have a high probability of being exceeded, the atmospheric noise measurements parallel those for thermal noise; this is characteristic of a phenomenon consisting of a large number of overlapping pulses, no one of which contributes a significant proportion of the total energy. At the high voltages, however, which have a low probability of being exceeded, the measurements depart radically from the shape of the thermal noise curve, in the form of a much higher probability of exceeding the voltage levels in the range of probabilities of 0.3 and below. Oscillograms of atmospheric noise show that the high voltage levels are attained by occasional noise pulses which greatly exceed the general level of the noise [Yuhara, Ishida, and Higashimura, 1956] and that the pulse shape is that of the impulse response of the receiver. These strong pulses occur infrequently and two such pulses very rarely overlap.

3. Probabilities Associated With Impulses

The effect of bandwidth changes on the probabilities associated with noise impulses can be calculated by considering the effect of bandwidth changes on the usual impulse response of the filter. The effect of increasing the bandwidth is to cause the impulse response to become shorter in time, and higher in amplitude [Guillemin, 1956]. More specifically, if the network characteristics are changed in such a way that the shape of the impulse response is preserved while the bandwidth is multiplied by a factor B , the voltage scale of the impulse response will be multiplied by a factor B and the time scale by a factor $1/B$, as illustrated in figure 2 for $B=2$. This relationship also holds for the envelope of the response of a band-pass circuit whenever the circuit possesses a low pass analog, as is normally the case with receiver circuits [Aigrain, Teare, and Williams, 1949; Guillemin, 1953]. Further, the probabilities associated with the impulse response are determined by the time scale; for example, the probability that a voltage level of one will be exceeded by the narrow band response is determined by the ratio of the time τ to the total observation time. Because of the relationship between changes in the voltage and time scales, the doubled bandwidth impulse response exceeds a voltage level of two for a time of $\tau/2$, which represents precisely one-half of the probability corresponding to a time τ .

Thus the amplitude distribution of a short sample of noise which contained only one impulse would be determined by the time and voltage scales of that impulse response; if a particular voltage v is measured to have a probability P of being exceeded when a single impulse is observed through a network of bandwidth $\Delta\omega_1$, and simultaneously the impulse is observed through a network of bandwidth $\Delta\omega_2 = B\Delta\omega_1$, the voltage Bv will be measured to have a probability $(1/B)P$ of being exceeded. This relationship also holds for a noise sample which consists of a number

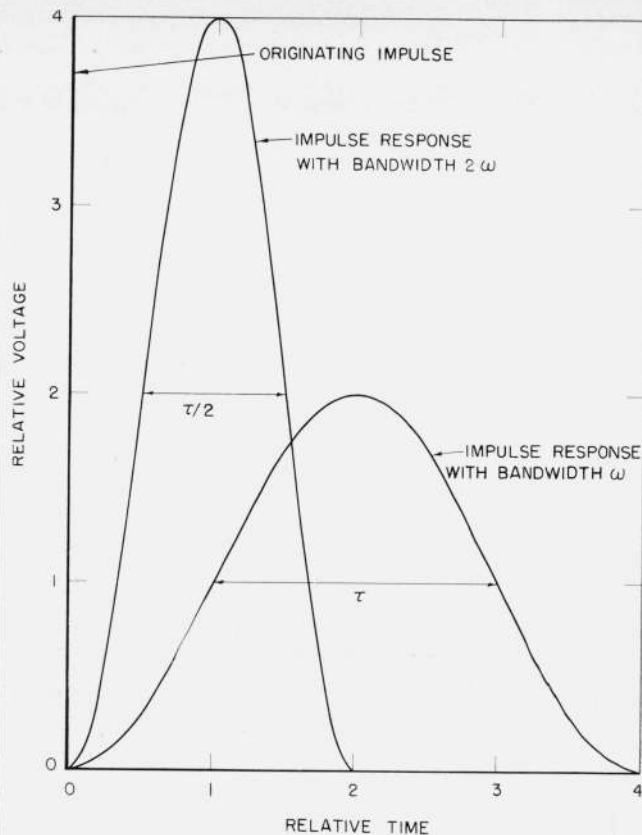


FIGURE 2. Envelope of band-pass impulse response for two bandwidths.

of impulses, provided that the response of the network to one impulse does not overlap the response to another.

These requirements are never exactly met in practice because of the exponential decay of physical networks and because of the presence of thoroughly overlapping low level noise. However, the high voltage end of the distribution of VLF atmospheric noise appears to represent an excellent approximation to the requirements. Figure 3 shows the high voltage portion of two representative sets of measurements at two bandwidths and also shows the results of translating the narrow-band measurements by the ratio of bandwidths to expected measurements at the wider bandwidth. It is evident that for both the low and high dynamic range noise conditions the points calculated from the narrow-band measurements agree with the measurements at the wider bandwidth for probabilities less than 0.01.

4. Mathematical Representation of the Noise

In dealing with a non-Gaussian random variable, it has proved profitable for some purposes to consider it as being generated as the output of a nonlinear resistance network which has a Gaussian input, even though the actual phenomenon may be very much

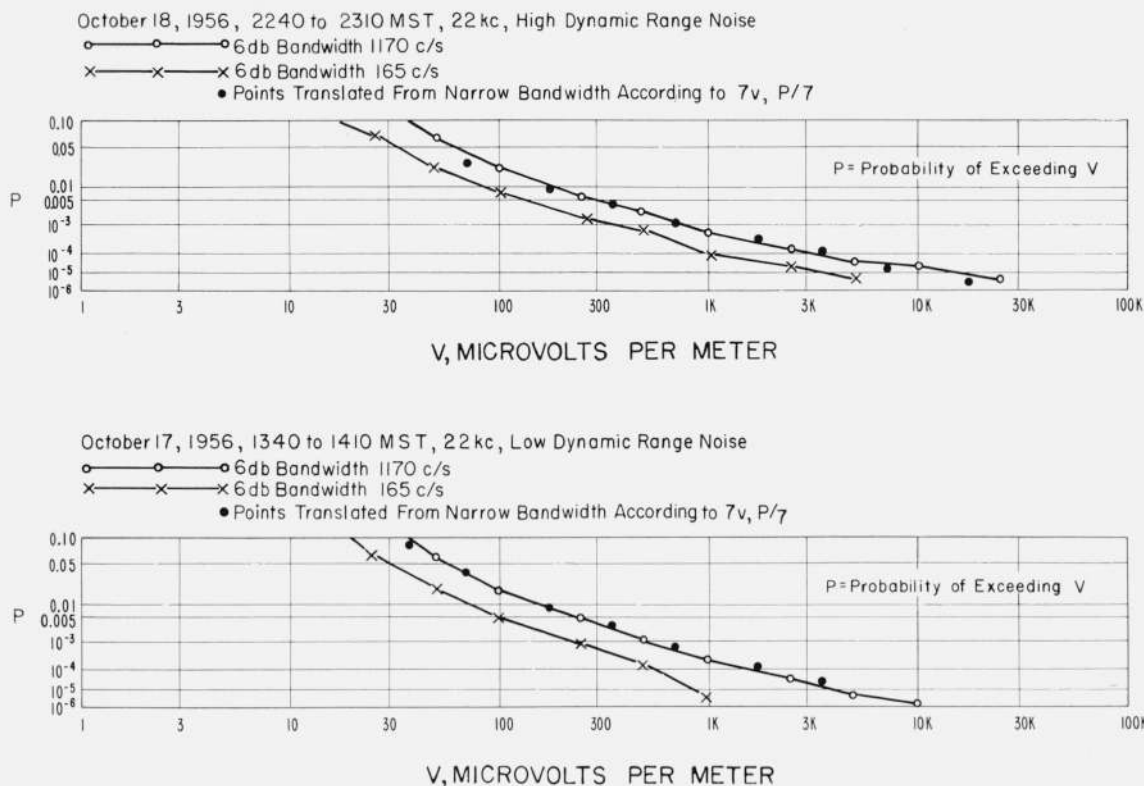


FIGURE 3. Atmospheric noise distributions showing effect of translating measurements made at a narrow bandwidth to expected values at a wider bandwidth.

different from this [Smith, 1959a and b]. In the situation being considered here where the envelope of the noise is the quantity of interest, we can represent the envelope of the actual noise as being obtained from an envelope detector having a Gaussian input, followed by a nonlinear resistance network. The justification for doing this is simply that the resulting probability distribution can represent the probability distribution of the actual phenomenon quite accurately, and the model proves to be a convenient one for the type of mathematical manipulations which are required.

A nonlinear network which can produce the correct probability distribution has a voltage transfer characteristic which is a three term polynomial of the form

$$v = a_1 \gamma + a_2 \gamma^{\frac{b+1}{2}} + a_3 \gamma^b \quad (1)$$

where a_1 , a_2 , a_3 , and b are chosen to match the atmospheric noise distribution under consideration; the probability that a voltage level v is exceeded at the output of the network is given by

$$P = e^{-\gamma^2}. \quad (2)$$

The variable γ may conveniently be considered just as a parametric variable, although it is the envelope voltage of a Gaussian variable having a variance of one-half.

Each term of the polynomial, if considered separately, plots as a straight line of log-log of probability versus logarithm of voltage, which are the coordinate scales used on the graphs of distributions in figures 1 and 3. The first term represents a distribution having complete overlapping, such as thermal noise; the second and third terms represent departures from this distribution. The third term of the polynomial, $a_3 \gamma^b$, is the dominant term at the high voltage, low probability end of the curve, when the phenomena forming the distribution appear to be strong, nonoverlapping pulses.

5. The Effect of Bandwidth Changes on the Mathematical Model

Since the third term of the polynomial is considered to represent nonoverlapping impulses, the effect of bandwidth changes can be obtained by the procedure described in section 3. That is, for an increase in bandwidth by a factor B , any point on the original line at voltage v and probability P is transformed to a voltage Bv at a probability P/B . After this is done, it is found that the points no longer lie on a straight line, but along a line having a slight curvature, as illustrated in figure 4 for an exponent of 8 and a bandwidth increase of ten times. The curvature introduced in this way is so slight, however, that the curve may be replaced by a line tangent to

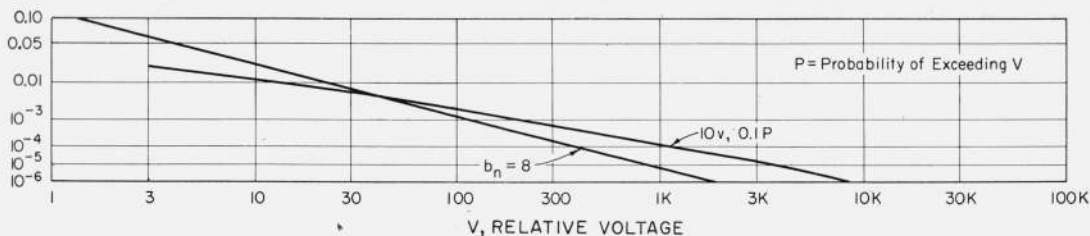


FIGURE 4. Curvature introduced by bandwidth transformation.

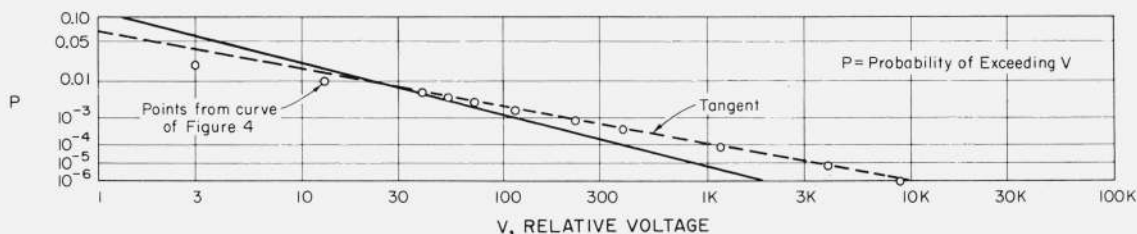


FIGURE 5. Tangent approximation to curve.

it at the point where $P=e^{-8}$; as is apparent from figure 5, this is an excellent approximation.

It is possible to derive a general formula for the effects of bandwidth changes on the exponent and the coefficient of the third term of the polynomial. For a bandwidth increase by a factor of B , the exponent b_w for the wider bandwidth is obtained from the exponent b_n for the narrow bandwidth by the relationship

$$b_w = \frac{8}{8 - L_n B} b_n \quad (3)$$

where $L_n B$ is the natural logarithm of B . The coefficient is obtained from

$$a_{3w} = a_{3n} B \left[(8 - L_n B) 8 \left(\frac{-8}{8 - L_n B} \right) \right]^{b_n} \quad (4)$$

where a_{3w} and a_{3n} are the coefficients for the wide and narrow bandwidths respectively. The derivation of these relationships is given in the appendix.

For the other terms of the probability function the effects of bandwidth changes are not as apparent as for the third term which describes the behavior at high voltages. The second term of the polynomial is important in the moderate voltage range where some overlapping of noise pulses occurs. For the values of exponents and coefficients which are required to match the mathematical model to the observed atmospheric noise conditions, it happens that the second moment of the distribution is almost entirely determined by the second and third terms of the polynomial. Since for normal communications bandwidths the total noise power received is directly proportional to the bandwidth, it is possible to adjust the second term to obtain the correct behavior for the second moment of the distribution.

The procedure is to calculate the changes in the a_3 coefficient and exponent b as described above, and to insert these into the expression for the mean squared voltage of this form of distribution, which is

$$\langle v^2 \rangle = a_1^2 + a_2^2 \Gamma \left(\frac{b+3}{2} \right) + a_3^2 \Gamma(b+1) + 2a_1 a_2 \Gamma \left(\frac{b+7}{4} \right) + 2a_1 a_3 \Gamma \left(\frac{b+3}{2} \right) + 2a_2 a_3 \Gamma \left(\frac{3b+5}{4} \right) \quad (5)$$

where $\langle v^2 \rangle$ is the mean squared voltage.

For a bandwidth increase by a factor of B , the mean squared voltage for the wide bandwidth is B times the mean squared voltage at the narrow bandwidth. With this and a value for a_1 , equation (5) can then be solved for the coefficient a_2 .

The first term of the polynomial, involving a_1 , represents a situation where complete overlapping occurs. The slope of a distribution represented by only this term does not change with bandwidth, but only its amplitude, as long as the complete overlapping is maintained. If this were the only term in the distribution, its amplitude would change precisely as the square root of the bandwidth. Since there are other terms present, however, there will be an interchange of energy between the various portions of the distribution, and the net effect will be that the amplitude of the first term will change more slowly than this; an increase according to the four-tenths power of the bandwidth appears to fit the available experimental data quite well.

These procedures work quite well with noise samples of low and moderate dynamic range, but an error appears when used with noise of high dynamic range, that is, values of b of about 11 or greater. This occurs because the mathematical

model being used is not sufficiently complex. With the very high dynamic range conditions, a substantial contribution to the integral for the mean squared voltage occurs at probabilities below 10^{-6} ; in this region the tangent line and the curve representing the distribution diverge significantly, causing considerable error in the evaluation of the mean squared voltage.

Under the high dynamic range conditions it seems appropriate to make the same transformation on the second term as on the third. Modification of the coefficient by some factor to compensate for the partial overlapping might be considered, but also considering the nature of the experimental data, that is, short samples of a nonstationary process, and also the relative unimportance of the second term, any refinement in the transformation seems unjustified.

6. Discussion

These somewhat arbitrary operations on the first and second terms, together with the accurate transformation for the high voltage end of the distribution where the third term is dominant, provide a method of describing what changes would be observed in the polynomial representation of the distribution of atmospheric radio noise amplitude when observed through different bandwidths. The results of carrying out the complete transformation on representative samples of high and low dynamic range noise are shown in figure 6 and figure 7. For the low dynamic range noise in figure 6, the a_2 coefficient was determined from the rms voltage relationship; for the high dynamic range noise in figure 7, it was determined by the transformation procedure for nonoverlapping pulses. It is apparent that these procedures provide good estimates of the distributions, and are useful and practical tools for use when more rigorous methods are not justified.

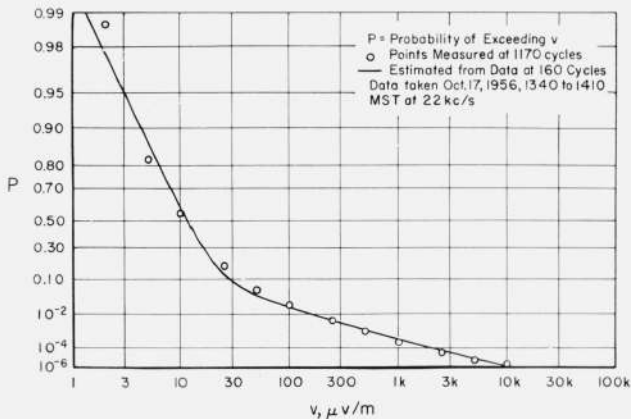


FIGURE 6. Low dynamic range atmospheric noise distribution measured at a wide bandwidth, and estimated distribution from simultaneous narrow bandwidth data.

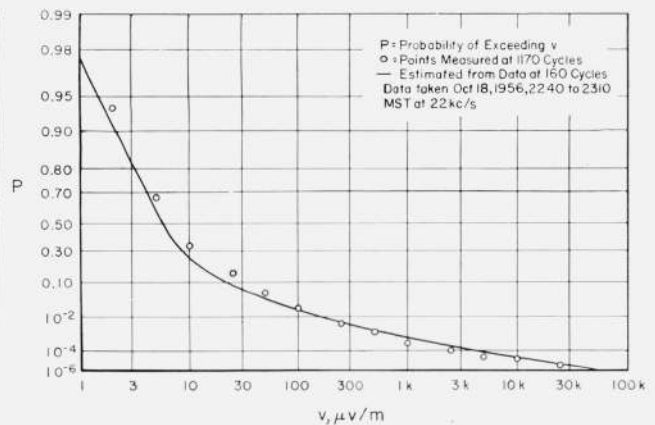


FIGURE 7. High dynamic range atmospheric noise distribution measured at a wide bandwidth, and estimated distribution from simultaneous narrow bandwidth data.

I wish to acknowledge the experimental data made available by A. D. Watt and E. L. Maxwell. L. P. Benedict provided valuable assistance with much of the numerical work.

7. Appendix: Variation of High Voltage Coefficient and Exponent

Consider a distribution having a form expressed by

$$v_1 = ay^b$$

$$P_1 = e^{-y^2} \quad (6)$$

when it is observed through a particular bandwidth. If this distribution is composed of nonoverlapping impulses, then when observed through a bandwidth B times larger, the voltages and probabilities will be related by the ratio of bandwidths according to

$$P_2 = \frac{P_1}{B}$$

$$v_2 = Bv_1 \quad (7)$$

where P_1 and v_1 are obtained at the first bandwidth and P_2 and v_2 at the second. From (6) and (7) we can write

$$\log(-\ln P_1) = \frac{2}{b} \log\left(\frac{v_1}{a}\right)$$

$$\log(-\ln BP_2) = \frac{2}{b} \log\left(\frac{v_2}{aB}\right) \quad (8)$$

We wish to develop an approximation to the relationship between v_2 and P_2 in the region of high voltages and low probabilities which will have the form

$$v_2 = aBC_1 y^{bC_2}$$

$$P_2 = e^{-y^2} \quad (9)$$

or

$$\log(-\text{Ln}P_2) = \frac{2}{bC_2} \log\left(\frac{v_2}{aBC_1}\right) \quad (10)$$

where C_1 and C_2 are constants to be determined. They may be evaluated by selecting two points on the P_2 versus v_2 relationship where the approximation is to be exact. Choosing the points $P_{2\alpha}$, $v_{2\alpha}$, and $P_{2\beta}$, $v_{2\beta}$, we obtain from (8)

$$\begin{aligned} v_{2\alpha} &= aB(-\text{Ln}BP_{2\alpha})^{\frac{b}{2}} \\ v_{2\beta} &= aB(-\text{Ln}BP_{2\beta})^{\frac{b}{2}}. \end{aligned} \quad (11)$$

Now in the approximation,

$$\begin{aligned} \log(-\text{Ln}P_{2\alpha}) &= \frac{2}{bC_2} \log\left(\frac{v_{2\alpha}}{aBC_1}\right) \\ \log(-\text{Ln}P_{2\beta}) &= \frac{2}{bC_2} \log\left(\frac{v_{2\beta}}{aBC_1}\right) \end{aligned} \quad (12)$$

C_1 may be eliminated from equations (12), obtaining

$$\log\left(\frac{\text{Ln}P_{2\alpha}}{\text{Ln}P_{2\beta}}\right) = \frac{2}{C_2b} \log\left(\frac{v_{2\alpha}}{v_{2\beta}}\right) \quad (13)$$

and from (11),

$$\frac{v_{2\alpha}}{v_{2\beta}} = \left(\frac{\text{Ln}BP_{2\alpha}}{\text{Ln}BP_{2\beta}}\right)^{\frac{b}{2}} \quad (14)$$

and from (13) and (14) we can obtain

$$C_2 = \frac{\log\left(\frac{\text{Ln}BP_{2\alpha}}{\text{Ln}BP_{2\beta}}\right)}{\log\left(\frac{\text{Ln}P_{2\alpha}}{\text{Ln}P_{2\beta}}\right)} \quad (15)$$

For the evaluation of C_1 , from (11) and (12) we can obtain

$$C_1 = \frac{(-\text{Ln}BP_{2\alpha})^{\frac{b}{2}}}{(-\text{Ln}P_{2\alpha})^2} = \frac{(-\text{Ln}BP_{2\beta})^{\frac{b}{2}}}{(-\text{Ln}P_{2\beta})^2} \quad (16)$$

Going back to the polynomial term itself, we can change the third term to read $a_{3w}y^{b_w}$, where

$$b_w = b_n C_2$$

and

$$a_{3w} = a_{3n} B C_1 \quad (17)$$

a_{3n} and b_n being the values observed at the narrow bandwidth.

A limiting value of C_2 is obtained as $P_{2\alpha}$ approaches $P_{2\beta}$ and this represents the approximation where the straight line is tangent to the curve. This limiting value may be found by application of

L'Hospital's rule, and is

$$C_2 = \frac{\text{Ln}P_{2\beta}}{\text{Ln}BP_{2\beta}} \quad (18)$$

If we use the tangent approximation and evaluate for

$$P_{2\alpha} = P_{2\beta} = e^{-8} = 0.000335$$

we obtain

$$b_w = C_2 b_n = \frac{8}{8 - \text{Ln}B} b_n \quad (19)$$

and

$$a_{3w} = a_{3n} B \left(\frac{8 - \text{Ln}B}{8C_2}\right)^{\frac{b_n}{2}} \quad (20)$$

Figure 5 shows this tangent line for an assumed b_n of 8 and B of 10, and also shows some points from the curve in figure 4. The difference between the straight line and the points from the curve is zero, of course, at $P=0.000335$, and increases slowly to about 1 db at $P=0.005$ and $P=10^{-6}$; it is evident that there is no significant difference between using the straight line and the curve, and the procedure using the tangent line provides a simple and accurate estimate of the changes in the high voltage end of the distribution curve.

8. References

- Aigrain, P. R., B. R. Teare, Jr., and E. M. Williams, Generalized theory of the band-pass low-pass analogy, Proc. IRE **37**, 1152-1155 (1949).
- Consultative Committee on International Radio, Revision of atmospheric radio noise data, CCIR Rpt. 65, International Telecommunication Union, Geneva (1957).
- Guillemin, E. A., Introductory circuit theory, p. 434 (John Wiley and Sons, Inc., New York, N.Y., 1953).
- Guillemin, E. A., The mathematics of circuit analysis, p. 526 (John Wiley and Sons, Inc., New York, N.Y., 1956).
- Hoff, R. S., and R. C. Johnson, A statistical approach to the measurement of atmospheric noise, Proc. IRE **40**, 185 (1952).
- Ragazzini, J. R., and G. F. Franklin, Sampled-data control systems, p. 261 (McGraw-Hill Book Co., Inc., New York, N.Y., 1958).
- Smith, O. J. M., Spectral output of piecewise linear non-linearity, A.I.E.E. Transactions, pt. 1, **78**, 543 (1959).
- Smith, O. J. M., Statistical spectral output of power law non-linearity, A.I.E.E. Transactions, pt. 1, **78**, 535 (1959).
- Watt, A. D., and E. L. Maxwell, Measured statistical characteristics of VLF atmospheric radio noise, Proc. IRE **45**, 55 (1957).
- Watt, A. D., R. M. Coon, E. L. Maxwell, and R. W. Plush, Performance of some radio systems in the presence of thermal and atmospheric noise, Proc. IRE **46**, 1914 (1958).
- Widrow, B., Propagation of statistics in systems, IRE Wescon Convention Record, pt. 2, 114 (1957).
- Yuhara, H., T. Ishida, and M. Higashimura, Measurement of the amplitude probability distribution of atmospheric noise, Journal of the Radio Research Laboratories, Tokyo, Japan, **3**, 101 (1956).